

# Numerical Techniques for the Analysis of Charge Transport and Electrodynamics in Graphene Nanoribbons

Invited Feature Article

Luca Pierantoni<sup>1,2,\*</sup> and Davide Mencarelli<sup>1</sup><sup>1</sup> Università Politecnica delle Marche, Ancona, Italy<sup>2</sup> INFN-Laboratori Nazionali di Frascati, Frascati, Italy

\* Corresponding author: l.pierantoni@univpm.it

Received 18 Oct 2012; Accepted 14 Nov 2012

© 2012 Pierantoni and Mencarelli; licensee InTech. This is an open access article distributed under the terms of the Creative Commons Attribution License (<http://creativecommons.org/licenses/by/3.0>), which permits unrestricted use, distribution, and reproduction in any medium, provided the original work is properly cited.

**Abstract** In this paper, we report on multiphysics full-wave techniques in the frequency (energy)-domain and the time-domain, aimed at the investigation of the combined electromagnetic-coherent transport problem in carbon based on nano-structured materials and devices, e.g., graphene nanoribbons.

The frequency-domain approach is introduced in order to describe a Poisson/Schrödinger system in a quasi static framework. An example of the self-consistent solution of laterally coupled graphene nanoribbons is shown.

The time-domain approach deals with the solution of the combined Maxwell/Schrödinger system of equations. The propagation of a charge wavepacket is reported, showing the effect of the self-generated electromagnetic field that affects the dynamics of the charge wavepacket.

**Keywords** Dirac Equation, Graphene Nanoribbon, Quantum Electrodynamics, Transmission Line Matrix

## 1. Introduction

The theoretical, scientific and technological relevance of carbon-based materials (carbon nanotubes, graphene) have been highlighted in a variety of works, both experimental and theoretical [1-11]. They are fated to become competitive and compatible with the established silicon technology for applications to electronics. The analysis of charge transport in carbon nano-structures can be carried out by discrete models, such as tight binding (TB), and continuous models, such as effective mass and  $k\cdot p$  approximations, which stem from the approximation of TB around particular points of the dispersion curves. These techniques are suited for the analysis of CNT/graphene/GNR in a variety of problems such as bending [17-18], lattice defects and discontinuities [14], and edge terminations [19-20]. However the latter methods require high computational resources, and can hardly include the effect of i) the self-generated electromagnetic field, ii) impinging external EM fields. Recently, we have introduced full-wave techniques (fig. 1) both in the frequency (energy)-domain [21-26], and the time-domain [28-36] for the investigation of new devices

based on carbon materials, namely carbon nanotube (CNT), multiwall (MW) CNT, graphene and graphene nanoribbon (GNR).

For both the approaches, the quantum transport is described by the Schrödinger equation or its Dirac-like counterpart, for small energies. The electromagnetic field provides sources terms for the quantum transport equations that, in turn, provide charges and currents for the electromagnetic field.

In this contribution, we report some new examples of self-consistent quasi-static calculations, where charges' transport is affected by the self-generated potential, in addition to the electrostatic potential applied by external electrodes, in a typical FET configuration [25,26]. Regarding the time-domain technique, we show the dynamics of a charge wavepacket from source to drain electrodes in a GNR realistic transistor environment.

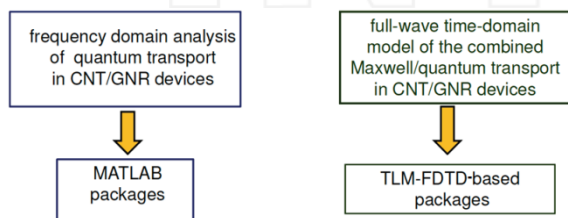


**Figure 1.** Frequency- and time-domain techniques.

### 2.1 Frequency-domain: Poisson-coherent transport

We perform the analysis of self-consistent charge transport by using a scattering matrix technique [24], which is physically equivalent to the Green's function approach, usually referred to as non-equilibrium Green's function (NEGF) method. In synthesis, each GNR port, seen as the termination of a semi-infinite waveguide, is described by means of a basis of electronic eigenfunctions, that, in turns, are solution of the GNR unit-cell under periodic condition. The analysis is fully self-consistent since the solution of the transport equation, and the solution of the Poisson equation for the electrostatic potential generated by the GNR charge density, are obtained by using an iterative approach. In the scattering-matrix approach, a multimode transmission matrix model of quantum transport allows easy simulation of very large structures, despite the possibly high number of electronic channels involved. In order to characterize a GNR, periodic along the  $z$ -direction, the Hamiltonian of the unit cell is appropriately rearranged by selecting three consecutive unit cells

$$H^l \psi_l + H^0 \psi + H^r \psi_r = E \psi \quad (1)$$

where  $\psi_l$ ,  $\psi_r$ ,  $\psi$ , are the wavefunctions of three consecutive unit cells and matrix  $H^l(H^r)$  denotes the

hopping elements of the Hamiltonian from a unit cell to the previous one from the left (right), and  $E$  is the injection energy.

In [24], we showed that fundamental physical constraints and consistence relations in quantum transport, such as reciprocity and charge conservation, correspond respectively to familiar reciprocity and power conservation in a microwave field. We emphasized that the proposed approach allows handling multiport graphene systems, where carriers can get into (and out of) many different physical ports, each characterized by their own chirality and possibly by a large number of virtual ports, i.e., electronic channels or sub-bands. Interesting results involve new concept-devices, such as GNR nano-transistors and multipath/multilayer GNR circuits, where charges are ballistically scattered among different ports under external electrostatic control. We developed a in-house solver for simulating CNT short-channel transistors, with a user friendly interface. The software, written in Matlab, has been, in particular, focused on the simulation of GNR short-channel transistors, as shown in fig. 1. In modelling the graphene-metal contact, we introduce a sort of metal doping of GNR, coherently with experimental observation; in fact, graphene over metal seems to preserve its unique electronic structure, and the metal just shifts the graphene Fermi level with respect to the conical point, by a fraction of eV [27]. Possibly, the metal contact opens just a small (tens to hundreds eV) bandgap.

### 2.2 Time-domain: Maxwell-coherent transport

In the time-domain, a full-wave approach has been introduced: the Maxwell equations, discretized by the transmission line matrix (TLM) method, are self-consistently coupled to the Schrödinger/Dirac equations, discretized by a proper finite-difference time-domain or a TLM scheme [28-29].

The goal is to develop a method that accounts for deterministic electromagnetic field dynamics, together with the quantum coherent transport in the nanoscale environment. In [29-30], we introduced exact boundary conditions that rigorously model absorption and injection of charge at the terminal planes, in a realistic field effect transistor environment.

Several examples of the electromagnetics/transport dynamics are shown in [28-29]. It is highlighted that the self-generated electromagnetic field may affect the dynamics (group velocity, kinetic energy, etc.) of the quantum transport. This is particularly important in the analysis of time transients and in describing the behaviour of high energy carrier bands, as well as the onset of non-linear phenomena due to external impinging

electromagnetic fields. For graphene/GNR, in the presence of an EM field, the Dirac equation reads:

$$i\hbar\left(\frac{\partial}{\partial t} + \frac{ie}{\hbar}\varphi\right)\psi_+ = \boldsymbol{\sigma} \cdot (\hat{\mathbf{p}} - q\mathbf{A})c\psi_- \quad (2)$$

$$i\hbar\left(\frac{\partial}{\partial t} + \frac{ie}{\hbar}\varphi\right)\psi_- = \boldsymbol{\sigma} \cdot (\hat{\mathbf{p}} - q\mathbf{A})c\psi_+$$

The solution of the Dirac/graphene equation (2) is the four component spinor complex wavefunction  $\psi(\mathbf{r},t)$ :

$$\boldsymbol{\psi}(\mathbf{r},t) = [\psi_1 \ \psi_2 \ \psi_3 \ \psi_4]^T = [\psi_+ \ \psi_-]^T \quad (3)$$

where  $\mathbf{A}$  and  $\varphi$  are vector and scalar potentials, directly related to the EM field through the appropriate gauge, e.g., the ‘‘Lorentz’’ gauge, and  $q$  is the electron charge;  $V_p$  is the static potential profile. In eq. (2),  $\boldsymbol{\sigma}$  are the Pauli matrices,  $\mathbf{p}$  is the canonical (linear) momentum,  $\mathbf{k}$  is the kinematic momentum, that, includes the EM field contribution:

$$\hat{\mathbf{p}} = -i\hbar\nabla \quad \hat{\mathbf{k}} = \hat{\mathbf{p}} - q\mathbf{A}(\mathbf{r},t) \quad (4)$$

The computational scheme develops as follows: i) the EM field is discretized by the Transmission Line Matrix method using the Symmetrical Condensed Node (SCN) approach. ii) Quantum phenomena are introduced in a subregion of the 3D-domain, e.g., a 1D-2D dimensional CNT region, described by the Schrödinger equation, and/or a 2D graphene/nanoribbon region, described by the Dirac equation. iii) At each time step, the Schrödinger/Dirac equation is solved by accounting for the quantum device boundary conditions, initial conditions (e.g., injected charge), and additional source terms constituted by the EM field, sampled in the domain of the quantum device(s). iv) From the wavefunction (charge) solution of the Schrödinger/Dirac equation, we derive the quantum mechanical (QM) current over the device domain. This current is a distribution of local sources for the EM field that is injected into the TLM nodes, located only on the grid points of the Schrödinger/Dirac equation domain. v) At the next time step  $t+1$ , the TLM method provides a new updated distribution of field values that are, again, sampled over the device domain, and so on, iteratively. In fig. 2, the scheme of the method is depicted in the case of graphene.

The reason for choosing TLM for the discretization of Maxwell equations has to be highlighted. Space-discretizing methods, like finite-difference time-domain (FDTD) and transmission line matrix (TLM) [38], are well-known techniques that allow the EM full-wave modelling of 3D structures with nearly arbitrary geometry for a wide range of applications from EM compatibility to

optics. FDTD is a more general technique, suited for discretizing different kinds of equations, e.g., parabolic, hyperbolic, etc. With respect to FDTD, TLM is directly related to the discretization of, mainly, hyperbolic equations (Maxwell, Dirac), but it has the advantages that each portion of the segmented space has an equivalent local electric circuit [38]. Moreover, TLM can easily incorporate external sources as equivalent voltage/current local generators.

In TLM, that is considered as the implementation of the Huygens principle, propagation and the scattering of the wave amplitudes are expressed by operator equations [38]. The latter property is well illustrated in the Symmetrical Condensed Node (SCN) formulation [38].

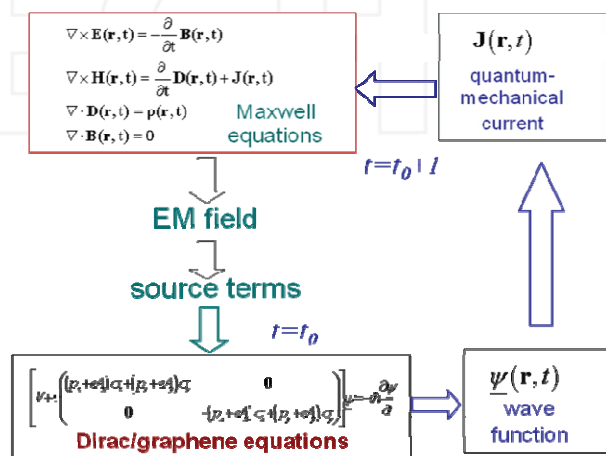


**Figure 2.** Concept of the full-wave time-domain technique. The electromagnetic field provides sources for the quantum device that, in turn, provides (quantum-mechanical) current sources for the electromagnetic field.

In [31-32], we explored the correlation between Dirac and Maxwell equations, in the time domain; transmission-line equations, valid for both EM and quantum current are derived. This is a step forward toward an effective integration of the Dirac theory in the numerical simulation of EM field problems.

In [33], we presented, for the first time, a TLM condensed node scheme for solving the Dirac equation in 2D graphene. This scheme satisfies the standard charge conservation requirement and allows adopting boundary conditions for graphene circuits.

The correlation between the graphene/Dirac equation and its self-consistent symmetrical condensed node - transmission line matrix formulation is highlighted. This concept, in turn, is related to the generalized Huygens principle for the Dirac equations.

The above technique has been already used for the investigation of realistic and intriguing applications in

novel areas, bridging nanoscience and engineering applications. We could define this research area as “radio-frequency nanoelectronic engineering”, [39-40].

In [34], we analyse the idea of realizing a harmonic radio-frequency identification (RFID), based on “tag on paper” with embedded graphene as a frequency multiplier.

In [35-36], we introduce a model for the metal-carbon contact. The metal-carbon transition is one of the most challenging and not completely understood problems that limits production and reproducibility of nanodevices, arising due to the difficulty of engineering the contact resistance between metal and nano-structures.

### 3. Results

#### 3.1 Frequency-domain: Schrödinger-Poisson

In order to show the potentialities of our approaches, in the following we show the comparison between the potential distributions in a region occupied by two laterally coupled GNR. The coupling takes place by means of the Coulomb interaction. The schematic view of the device under study is shown in fig. 3: two semiconducting GNRs connect the source and drain of a FET-like device.

A potential difference of 0.1 V is applied between drain and source; the source is assumed at 0 V, equipotential with the lateral gate (G). The nanoribbons are about 2.2 nm wide and the area of the square “window” delimited by the electrodes is 20x20 nm<sup>2</sup>.

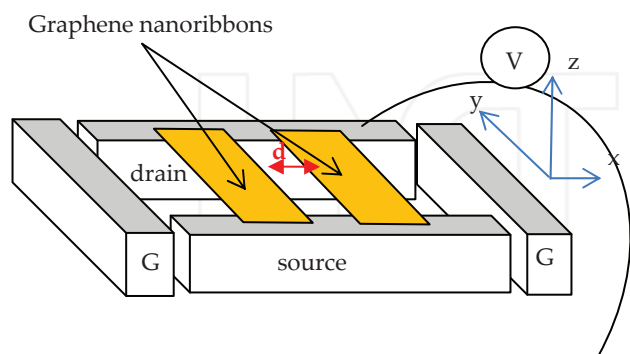
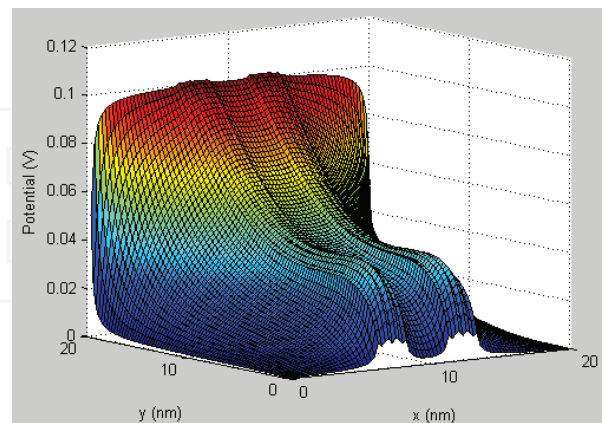


**Figure 3.** A two-channel GNR-FET;  $d$  is the distance between the two GNR channels.

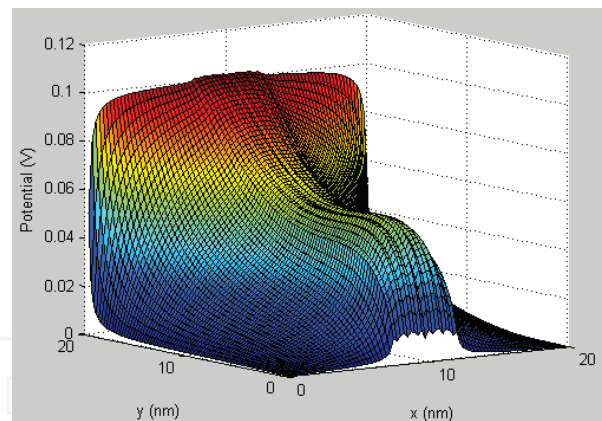
In the following, we report the numerical result obtained after numerical convergence, expressing the self-consistent potential in the plane of the nanoribbons. We somehow exaggerated the effect of the metal doping by assuming a 2.9 eV shift of the Dirac point, in order to place the Fermi level about 0.7eV above the band gap, and to have appreciable charge injection from the metal to nanoribbon “bridges”. In practice, a smaller doping

can still imply a strong effect when wider GNR, i.e., smaller band gaps, are considered.

It is noted that the self-consistent potential of fig. 4b is strongly different from the potential of fig 4a; as largely expected, changing the distance between the GNR does not simply imply a potential “composition” following a superposition of effects - the iterative process develops very differently in the two cases and the final results are not easily predictable.



a)



b)

**Figure 4.** Self-consistent potential for different distances of the two coupled GNR channels: a)  $d=2.4$  nm b)  $d=0.15$  nm.

#### 3.2 Time-domain: Dirac-Maxwell

We analyse the space-time evolution of a Gaussian charge wavepacket  $|\psi|^2$  with a broad energy band (up to 1 eV), propagating on a “metallic” GNR (150x5 nm), as shown in fig. 5. We consider the GNR in a realistic FET environment, with two metallic source-drain electrode contacts. In order to model the injection-absorption of charge, we apply absorbing boundary conditions as in [29]. In fig. 6 (a), we show the charge wavepacket evolution after  $t=0$ ,  $t=20$ ,  $t=50$ ,  $t=100$  fs, respectively. The correspondent transversal and longitudinal current components are reported in Fig. 6 (b), for  $t=20$ ,  $t=50$  fs.

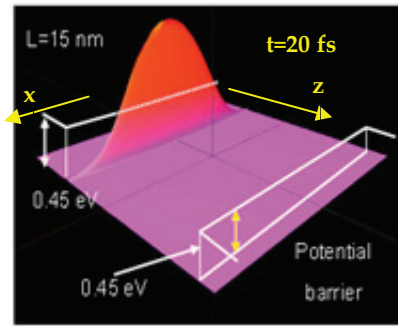


**Figure 5.** Propagation of a charge wavepacket in the presence of a static potential barrier, with  $E=0.45$  eV.

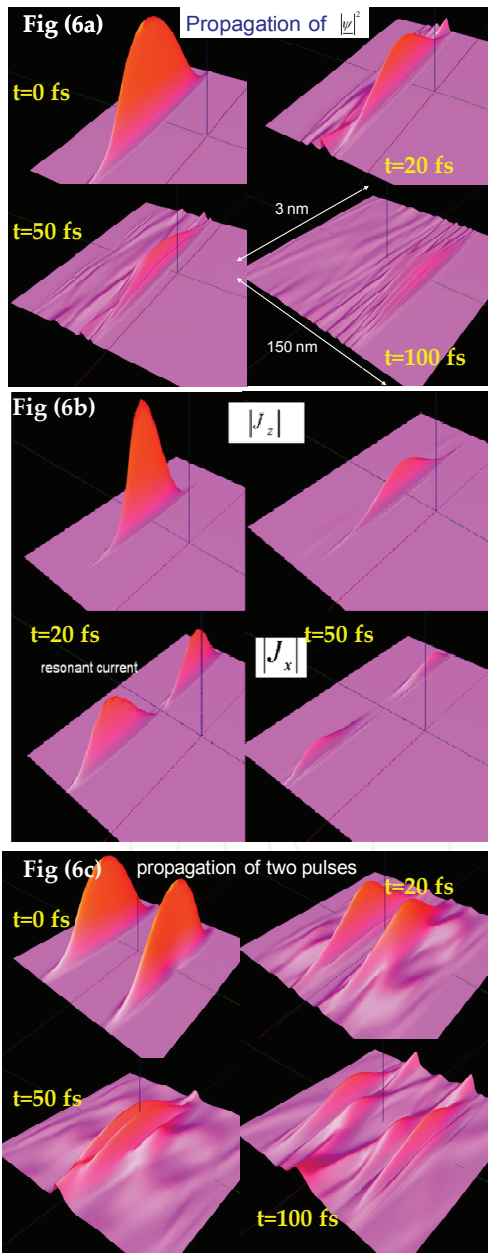


**Figure 6.** Time-evolution of the wavepacket (a). Transversal and longitudinal currents (b). Two launched pulses (c) from the source and drain terminals.

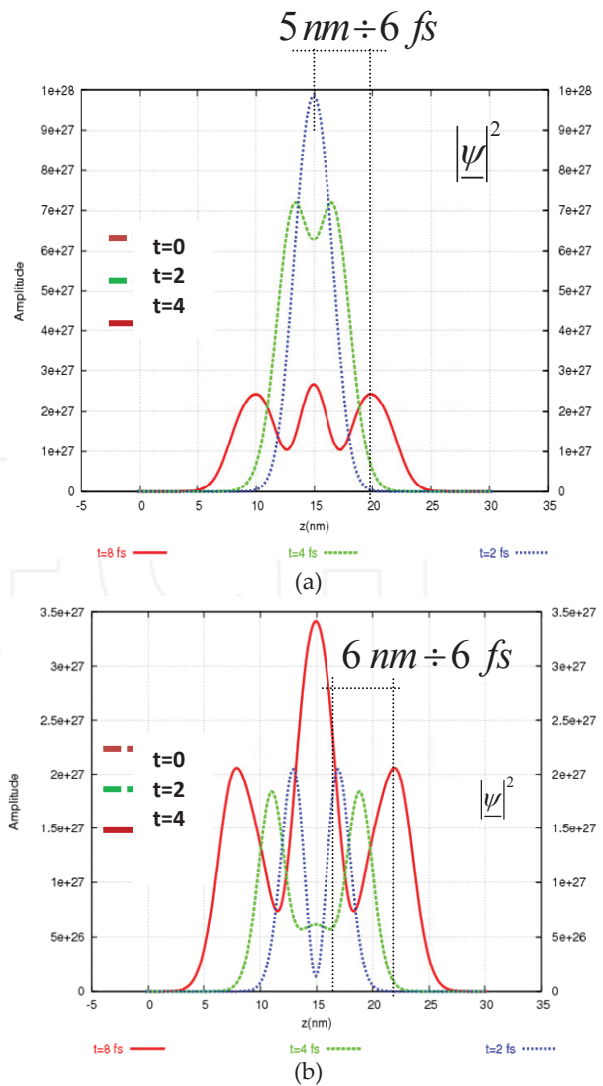


**Figure 7.** Spatial distribution of a charge wavepacket at  $t=0$ ,  $t=2$ ,  $t=4$  fs. (a): only the Dirac equation is solved. (b): the coupled Dirac-Maxwell system is computed.

In the same figure, (c), we show the propagation of two pulses launched through the source and drain electrodes, for  $t=0$ ,  $t=20$ ,  $t=50$ ,  $t=100$  fs.

We then consider the presence of a potential barrier of 0.45 eV with respect to bounding materials (e.g., metal contacts). In fig. 7, we plot the spatial, longitudinal distributions of the charge wavepacket in three different time-steps,  $t=2$ , 4, 8 fs, respectively.

The core point is that in one case (fig.7, a), we solve only the Dirac equation and do not consider

the self-induced EM field, whereas in the other case (fig.7, b), we consider the coupled Dirac-Maxwell system.

We observe that, depending on the initial energy of the charge wavepacket, the self-induced electromagnetic field affects the propagation characteristics.

This is evident by following the dynamics of the (squared) wavefunction with and without the “self-generated” electromagnetic field. For example, the distribution of the peaks (points of maxima) is different in the former and in the latter cases. Physically, the kinematic momentum,  $\mathbf{k}$ , provides the EM field contribution to the kinetic energy (3) of the Dirac equation. The quantum-mechanical current, in turn, provides current sources for the electromagnetic field.

This effect, as a result of this phenomenon, would be even more evident, and also enhanced in the presence of an additional external impinging EM field.

#### 4. Conclusions

We reported on multiphysics full-wave techniques in the frequency (energy)-domain and the time-domain, aimed at the investigation of the combined electromagnetic-coherent transport problem in graphene nanoribbons.

In the frequency-domain, we describe a Poisson/Schrödinger system in a quasi static framework.

In the time-domain, we deal with the solution of the combined Maxwell/Schrödinger coupled equations.

In the frequency-domain, we analyse the field coupling of graphene nanoribbons in an FET d configuration

In the time-domain, we present the charge wavepacket propagation, showing the effect of the self-generated electromagnetic field, that affects the dynamics of the charge wavepacket.

#### 5. References

- [1] Z. Chen, Y.-M. Lin, M. J. Rooks and P. Avouris, vol. 40, Issue 2, pages 228-232, Dec. 2007.
- [2] M. Y. Han et al., *Phys. Rev. Lett.* 98, 206805, 2007.
- [3] X. Li, et al., *Science* 319, 1229, 2008.
- [4] C. Stampfer, J. Güttinger, S. Hellmüller, F. Molitor, K. Ensslin, and T. Ihn, *Phys. Rev. Lett.* 102, 056403, 2009.
- [5] X. Liu, J. B. Oostinga, A. F. Morpurgo, L. M. K. Vandersypen, *Phys. Rev. B* 80, 121407, 2009.
- [4] C. Stampfer, et al., *Phys. Re Lett.* 102, 056403, 2009.
- [6] K. Wakabayashi and M. Sigrist, *Phys. Rev. Lett.* 84, 3390–93, 2000.
- [7] S. Souma, M. Ogawa, T. Yamamoto and K. Watanabe, *J. of Computational Electronics*, vol. 7, n.3, 390-393, 2008.
- [8] Guo J., Datta S. and Lundstrom M. (2004), A numerical study of scaling issues of Schottky-barrier of carbon nanotube transistors, *IEEE Transaction on Electron Devices*, vol. 51, n. 2, pages: 172-177
- [9] Lin Y.-M., et al., High Performance Dual-Gate Carbon Nanotube FETs with 40-nm Gate Length, *IEEE Electr. Dev. Letters*, vol. 26.
- [10] Guo J., et al. M. (2004), A numerical study of scaling issues of Schottky-barrier of carbon nanotube transistors, *IEEE Transaction on Electron Devices*, vol. 51, n. 2, pages: 172-177.
- [11] A. Kand et al., (2005), Leakage and performance of zero-Schottky-barrier of carbon nanotube transistors, *Jour. of App. Physics*, vol. 98.
- [12] L. Brei, H. A. Fertig, Electronic States of Graphene Nanoribbons, *cond-matt. 0603107*, pp. 1-5, Mar 2006.
- [13] G. Giovannetti et al., Substrate induced band-gap on hexagonal boron nitride: *Ab initio* density functional calculations, *Phys. Rev. B* 76, 073103' pp. 1-4, (2007).
- [14] G. Fiori, Negative Differential Resistance in mono and bilayer graphene p-n junctions *IEEE Trans. Elec. devices*, vol. 55, n. 9, Sept. 2008.
- [15] Z. F. Wang, R. Xiang, Q. W. Shi, J. Yang, X. Wang, J. G. Hou and J. Chen, *Phys. Re B* 74, 125417, 2006.
- [16] T. Ando, *Physical Review B* 44, 8017, 1991.
- [17] E. Castro, N. M. R. Peres and J. M. B. Lopes dos Santos, *Phys. Stat. Sol. (b)* 244, , 2311–2316, 2007.
- [18] A. Rycerz, Nonequilibrium valley polarization in graphene nanoconstrictions, *Cond-mat.*, 0710.2859v2, pp.1-10, 2007.
- [19] A. Akhmerov, C. W. J. Beenakker, Boundary conditions for Dirac fermions on a terminated honeycomb lattice, *Cond-mat.*, 0710.2723v1, pp. 1-10, 2008.
- [20] G. Lee and K. Cho, *Phys. Rev. B*, Apr. 10, 2009.
- [21] D. Mencarelli, L. Pierantoni, T. Rozzi, Optical Absorption of Carbon Nanotube Diodes: Strength of the Electronic Transitions and Sensitivity to the Electric Field Polarization, *Journal of Applied Physics*, vol. 103, Issue 6, pp.0631-03, March 2008.
- [22] D. Mencarelli, T. Rozzi, C. Camilloni, L. Maccari, A. Di Donato, L. Pierantoni, Modeling of Multi-wall CNT Devices by Self-consistent Analysis of Multi-channel Transport, *IOP Science Nanotechnology*, vol. 19, Number 16, April 2008.
- [23] D. Mencarelli, T. Rozzi, L. Pierantoni, Coherent Carrier Transport and Scattering by Lattice Defects in Single- and Multi-Branch Carbon Nanoribbons, *Physical Review B*, vol.77, pp.1954351-11, May 2008.
- [24] D. Mencarelli, T. Rozzi, L. Pierantoni, Scattering matrix approach to multichannel transport in many lead graphene nanoribbons, *IOP Science Nanotechnology*, vol. 21, no.15, March 2010, pp. 5570-15580.
- [25] D. Mencarelli, L. Pierantoni, A. Di Donato, T. Rozzi, Self-consistent simulation of multi-walled CNT nanotransistors, *Int. Journal of Micr. and Wireless Technologies*, vol. 2, no. 5, pp 453-456, Dec. 2010.
- [26] D. Mencarelli, L. Pierantoni, M. Farina, A. Di Donato, T. Rozzi, A multi-channel model for the self-consistent analysis of coherent transport in graphene nanoribbons, *ACS Nano*, vol. 5, Issue 8, August 2011. pp. 6109-6128.

- [27] A.L. Walter, et al., Electronic structure of graphene on single-crystal copper substrates, *Phys. Rev. B* 84, 195443, 2011.
- [28] L. Pierantoni, D. Mencarelli and T. Rozzi, A new 3D-Transmission Line Matrix Scheme for the Combined Schrödinger-Maxwell Problem in the Electronic/Electromagnetic Characterization of Nanodevices, *IEEE Trans. on Microwave Theory and Techniques*, vol. 56, no. 3, March 2008, pp.654-662
- [29] L. Pierantoni, D. Mencarelli, and T. Rozzi, Boundary Immittance Operators for the Schrödinger-Maxwell Problem of Carrier Dynamics in Nanodevices, *IEEE Trans. Microw. Theory Tech.*, vol. 57, issue 5, pp. 1147-1155, May 2009.
- [30] L. Pierantoni D. Mencarelli, T. Rozzi, Modeling of the Electromagnetic/Coherent Transport Problem in Nano-structured Materials, Devices and Systems Using Combined TLM-FDTD techniques, *Microwave Symposium Digest, 2011 Int. Microwave Symposium*, Baltimore, MA, USA, June 5-10, 2011, pp. 1-4.
- [31] T. Rozzi, D. Mencarelli, L. Pierantoni, Deriving Transmission Line Models and E.M. Fields from Dirac Spinor in Time Domain, *IEEE Trans. Microwave Theory Techn., Special Issue on RF Nanoelectronics*, vol. 59, no.10, Oct. 2011, pp. 2587-2594.
- [32] T. Rozzi, D. Mencarelli, L. Pierantoni, Towards a Unified Approach to Electromagnetic Fields and Quantum Currents From Dirac Spinors, *IEEE Transactions on Microwave Theory and Techniques, Special Issue on RF Nanoelectronics*, vol. 59, no.10, Oct. 2011, pp. 2587-2594.
- [33] D. Mencarelli, L. Pierantoni T. Rozzi, Graphene Modeling by TLM approach, *Microwave Symposium Digest, 2012 Int. Microwave Symposium, Montreal, QC, Canada*, June 17-22, 2012, pp. 1-3.
- [34] L. Pierantoni, D. Mencarelli, T. Rozzi, F. Alimenti, L. Roselli, P. Lugli, Multiphysics analysis of harmonic RFID tag on paper with embedded nanoscale material, *Proceedings of the 5th European Conference on Antennas and Prop.*, Rome, Italy, April 11-15, 2011.
- [35] L. Pierantoni D. Mencarelli, T. Rozzi, Full-Wave Techniques for the Multiphysics Modeling of the Electromagnetic/Coherent-Transport Problem Graphene Nanodevices, *Proceedings of the IEEE International Symposium on Antennas and Propagation (AP-S) and USNC-URSI National Radio Science Meeting*, Chicago, IL, USA, July. 8-14, 2012.
- [36] L. Pierantoni D. Mencarelli, T. Rozzi, Advanced Techniques for the Investigation of the Combined Electromagnetic-Quantum Transport Phenomena in Carbon Nanodevices, *Proc. of the Int. Conference on Electromagnetics in Advanced Applications (ICEAA) 2012-IEEE APWC 2012-EEIS 2012*, Cape Town, South Africa, Sept. 2-7, 2012, pp. 873-876.
- [37] G. Vincenzi, G. Deligeorgis, F. Coccetti, M. Dragoman, L. Pierantoni, D. Mencarelli, R. Plana, Extending ballistic graphene FET lumped element models to diffusive devices, *Solid-State Electronics*, vol. 76, Oct. 2012, pp. 8-12.
- [38] L. Pierantoni, A. Massaro, T. Rozzi, Accurate Modeling of TE/TM Propagation and Losses of Integrated Optical Polarizer, *IEEE Trans. Microw. Theory Tech.*, vol. 53, no.6, June 2005, pp. 1856-1862.
- [39] L. Pierantoni, RF Nanotechnology - Concept, Birth, Mission and Perspectives, *IEEE Microwave Magazine*, vol. 11, no. 4, pp. 130-137, June 2010.
- [40] L. Pierantoni, F. Coccetti, P. Lugli, S. Goodnick, Guest Editorial, *IEEE Transactions on Microwave Theory and Techniques, Special Issue on RF Nanoelectronics*, vol. 59, no.10, Oct. 2011, pp. 2566-2567, vol. 59, no.10, Oct. 2011, pp. 2566-2567.

INTECH